J Fluoresc (2011) 21:1721–1728
DOI 10.1007/s10895-011-0867-6

ORIGINAL PAPER

A Comprehensive Therotical Investigation of Intramolecular Proton Transfer in the Excited States for Some Newly-designed Diphenylethylene Derivatives Bearing 2-(2-Hydroxy-Phenyl)-Benzotriazole Part

Hongru Li · Lanying Niu · Xiaofang Xu · Shengtao Zhang · Fang Gao

Received: 30 October 2010 / Accepted: 13 February 2011 / Published online: 3 March 2011
© Springer Science+Business Media, LLC 2011

Abstract This article presents a comprehensive therotical investigation of excited state intramolecular proton transfer (ESIPT) for some newly-designed diphenylethylene derivatives containing 2-(2-hydroxy-phenyl)-benzotriazole moiety with various substituted groups. The calculation shows the structural parameters and Mulliken charges of phototautomers enol (E) and keto (K) of these compounds exhibit no or tiny changes from S_0 to S_1. The calculated results suggest that HOMO and LUMO + 1 of the compounds displays excellent overlapping nature, and thus the absorption and emission could be from the electron transition of HOMO→LUMO + 1. The electron density distribution in the frontier orbital of E and K are influenced remarkably by various substituted groups in S_0 and S_1 states. Electron density distribution deficiency in 2-(2-hydroxy-phenyl)-benzotriazole part is observed in L + 1 for these derivatives. The calculation also suggests the potential energy curves of ESIPT are shown to be a strong relationship with electron donor-acceptor groups. The absorption spectra, normal emission spectra and ESIPT spectra of the derivatives were also calculated.

Keywords ESIPT · Energy level curve · 2-(2-Hydroxyl-phenyl)-benzotriazole · Chromophore · Electron donor-acceptor groups

H. Li (✉) · L. Niu · X. Xu · S. Zhang · F. Gao (✉)
College of Chemistry and Chemical Engineering,
Chongqing University,
Chongqing 400044, China
e-mail: hhongruli1972@gmail.com
e-mail: fanggao1971@gmail.com

Introduction

ESIPT is a significantly important phenomenon in chemical and biological systems, for example phototautomerization occurs in DNA base pair [1, 2], and it attracts numerous experimental and theoretical interests [3–8]. Generally, enol (E)—keto (K) phototautomerism takes place mainly via five- [9], six- [10], or rarely seven-member [11] quasi transition state in the excited state of ESIPT molecule, and so dual fluorescence bands could be observed normally as the absorption is from E→E* and emission is from K*→K. Hence, the second emission band is characterized with huge Stokes red-shift, which has been found in a wide range of applied fields, such as photochromic dyes [12], laser dyes [13], fluorescent probes [14], sensors [15], organic electro-luminescence optical materials [16] and so on [17]. Consequently, this inspires scientists to search for various ESIPT organic compounds. ESIPT depends on the energy level changes of E*→K*, and only small energy barrier or even barrierless is allowed. This could be the major reason why the most ESIPT molecules reported were characterized with small molecular sizes.

We propose herein that it could be an efficient strategy to develop new large size ESIPT molecules if ESIPT moiety is attached to chromophore group via covalent bond. If ESIPT is correlated to chromophore part, the potential energy curves of the internal proton transfer could be tuned by the variation of chromophore part. This means that the variation of electron donor or acceptor groups in chromophore part could be emploed to tune the potential energy curves of ESIPT. To our limited knowledge, no detail theoretical investigation has been performed for such large organic

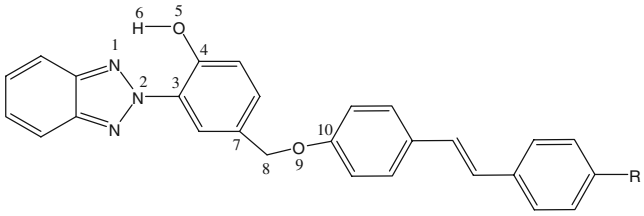

C1: R:H , **C2**: R: F, **C3**: $N(CH_3)_2$, **C4**: R: $N(Ph)_2$

Fig. 1 Chemical structures of diphenylethylene derivatives containing 2-(2-hydroxy-phenyl)-benzotriazole derivatives **C1** to **C4**

compounds because the complicated and time-exhausting computation is always a huge challenge.

In order to reveal the interrelationship between the chromophore part and ESIPT in theory, **C1**~**C4** (Fig. 1) were newly designed by the covalent linkage of 2-(2-hydroxy-phenyl)-benzotriazole and diphenylethylene part containing various electron donor or acceptor groups (H, F, dimethylamino, diphenylamino) . We have two main reasons to investigate ESIPT of such derivatives in theory: (1) 2-(2-hydroxy-phenyl)-benzotriazole could undergo ESIPT easily via energy barrierless [18]. Hence, such molecules could act as excellent models to survey the effect of chromophore part on the internal proton transfer path in the excited states. (2) the emission of the derivatives could be enhanced by chromophore part. Of particular interests of this article is trying to understand theoretically the effect of electron donor or acceptor in chromophore part on ESIPT. The calculation would give the guidance to develop new various large ESIPT molecules.

Calculation Method

The calculations were performed by means of the Gaussian 03 program package [19]. The geometry optimization of phototautomers (E and K) in the ground electronic state (S_0) was carried out with HF (Hatree-Fock) method and at DFT (density functional theory) level using the B3LYP method both [20–22], while CIS has been employed to optimize the geometries of S_1 state of the phototautomers of **C1** to **C4** (Fig. 1).

Table 1 Main structural parameters of phototautomers of **C1**, **C2**, **C3** and **C4**

Parameters	E_0	E	E^*	K^*	E_0	E	E^*	K^*
	C1				C2			
N_1–N_2	1.370	1.330	1.330	1.375	1.369	1.330	1.330	1.375
N_2–C_3	1.421	1.421	1.420	1.383	1.421	1.421	1.420	1.382
C_3–C_4	1.414	1.391	1.391	1.459	1.414	1.391	1.391	1.460
C_4–O_5	1.368	1.361	1.360	1.268	1.368	1.360	1.360	1.268
O_5–H_6	1.001	0.958	0.958	1.841	1.001	0.958	0.958	1.838
N_1–H_6	1.731	1.898	1.897	1.007	1.731	1.897	1.897	1.005
N_1–O_5	2.599	2.668	2.667	2.595	2.600	2.667	2.667	2.703
N_1–H_6–O_5	142.78	135.61	135.60	128.91	142.76	135.61	135.56	129.07
N_1–N_2–C_3–C_4	0.34	0.77	0.82	−19.27	0.31	0.72	0.81	17.40
C_3–C_4–O_5–H_6	−0.42	−0.81	−0.85	13.58	−0.38	−0.76	−0.83	−12.39
C_7–C_8–O_9–C_{10}	177.25	178.84	178.71	−179.23	177.27	178.88	178.66	−179.83
	C3				C4			
N_1–N_2	1.369	1.330	1.330	1.378	1.369	1.330	1.330	1.375
N_2–C_3	1.421	1.421	1.421	1.384	1.421	1.421	1.421	1.383
C_3–C_4	1.424	1.391	1.392	1.459	1.414	1.391	1.391	1.459
C_4–O_5	1.369	1.361	1.361	1.268	1.368	1.361	1.361	1.268
O_5–H_6	1.001	0.958	0.958	1.844	1.001	0.958	0.958	1.841
N_1–H_6	1.732	1.898	1.897	1.008	1.733	1.898	1.897	1.007
N_1–O_5	2.600	2.668	2.668	2.597	2.601	2.668	2.668	2.595
N_1–H_6–O_5	142.77	135.63	135.65	128.82	142.72	135.61	135.63	128.92
N_1–N_2–C_3–C_4	0.18	0.77	0.77	−20.53	0.26	0.77	0.79	−19.25
C_3–C_4–O_5–H_6	−0.37	178.80	178.52	−179.20	−0.43	178.83	178.45	−179.21
C_7–C_8–O_9–C_{10}	176.73	−178.88	−175.15	−178.90	178.04	−179.17	180.00	−179.07

Bond lengths and angle in Angstroms and Degree

E_0 calculated with DFT/6-31G, E calculated with HF/6-31G, E^*, K^* calculated with CIS/6-31G

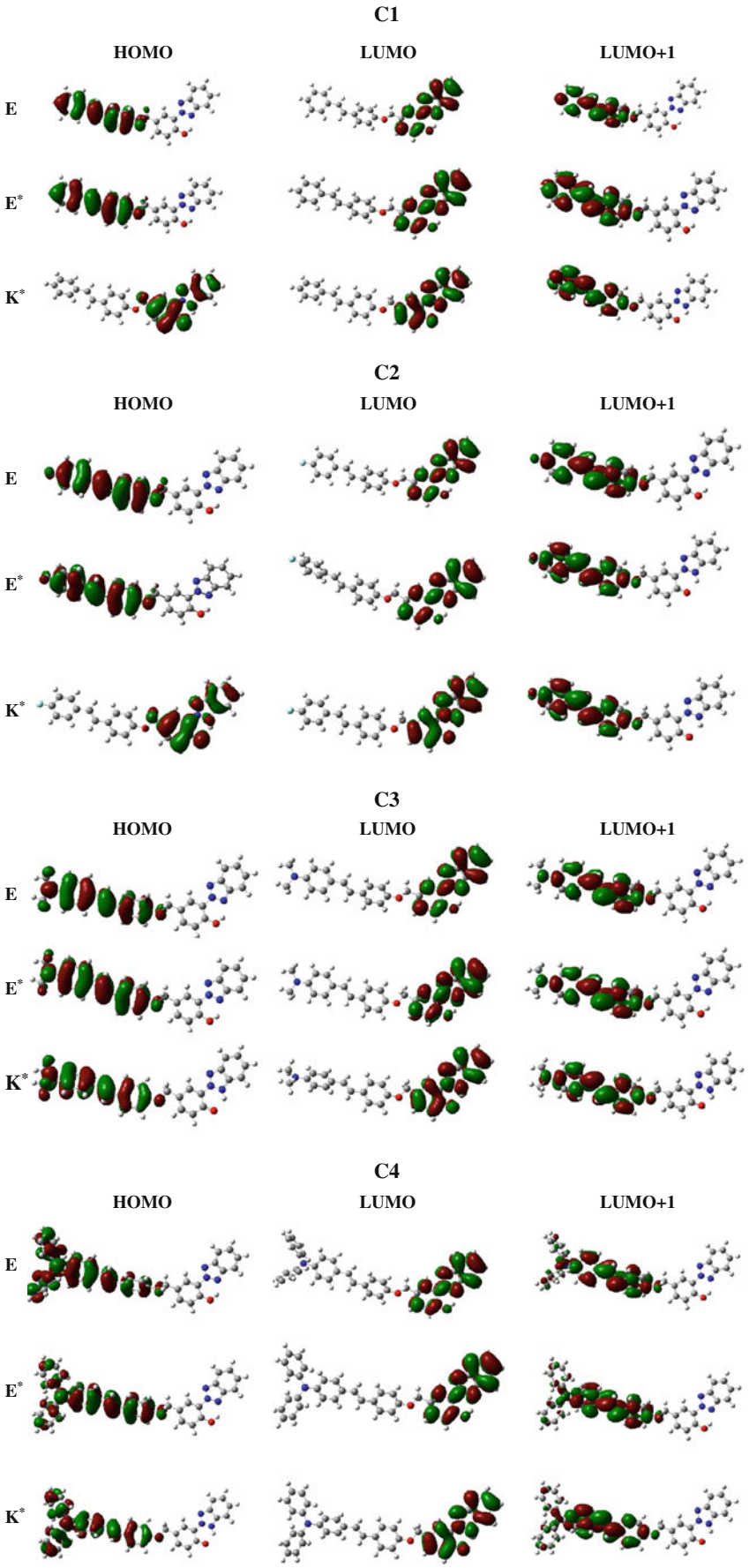

Fig. 2 Electron cloud density distribution of the frontier orbits of phototautomers of **C1** to **C4**

Table 2 Mulliken charge population for the active atoms of phototautomers of **C1** to **C4**

Compounds	Phototautomers	N_1/e	O_5/e	H_6/e
C1	E	−0.466	−0.570	0.335
	E^*	−0.467	−0.569	0.335
	K^*	−0.431	−0.644	0.320
C2	E	−0.466	−0.570	0.335
	E^*	−0.467	−0.569	0.335
	K^*	−0.432	−0.644	0.320
C3	E	−0.466	−0.571	0.334
	E^*	−0.466	−0.571	0.334
	K^*	−0.430	−0.645	0.320
C4	E	−0.370	−0.806	0.480
	E^*	−0.370	−0.806	0.480
	K^*	−0.637	−0.793	0.503

Although CIS method could produce reliable geometry and force-field, it predicts too high excitation energy (by *ca*. 1 eV) [23]. In order to correct the errors and introduce the dynamic electron correlation, DFT and TDDFT (Time-resolved DFT) were performed to calculate the energies of the HF and CIS optimized geometries in S_0 and S_1 state respectively, such as DFT//HF or TDDFT//CIS (denoted as single-point calculation//optimization method). TDDFT//HF and TDDFT//DFT were employed to calculate the absorption spectra, and Franck-Condon progression was calculated by TDDFT. TDDFT//CIS was used to analyze the energies and fluorescence spectra of the phototautomers. The calculated absorption spectra, normal fluorescence spectra of the normal emission and "abnormal" fluorescence spectra of tautomer species emission of each compound were obtained with the Lorenz broadening of the anterior twenty excitation energies and corresponding oscillator strengths with Swizard program [24, 25]. The peak wavelength of the spectrum is equal to the corresponding singlet-singlet strongest transition energy. The values of absorption refer to the vertical transition from the S_0 states to the Franck-Condon S_1 states, while the value from the S_1 states to the corresponding Franck-Condon S_0 state yields an assignment to fluorescence [26].

Results and Discussion

Structural Parameters and Mulliken Charge

Normally the molecular structure of a ESIPT exhibits large change as excitation. This means that the structural parameter changes of E and K in S_0 and S_1 could be employed to determine internal proton transfer in the excited state. We feel some surprised that the stable structure of K forms of the derivatives could not be obtained in S_0. In contrast, 2-(2-hydroxy-phenyl)-benzotriazole exhibits the stable K form in S_0 [18]. This indicates that the molecular size does have influence on ESIPT. CIS method in the excited state is equivalent to HF method in the ground state, hence, the results from CIS and HF are compared particularly herein. It is generally accepted that O–H distance will be enlarged and N–H distance will be reduced in the excited state of E form if ESIPT occurs. However, Table 1 shows that O5-H6 and N1-H6 distances of the phototautomers of the derivatives in S_0 and S_1 exhibit no change or very tiny change from E to E^*. This indicates that ESIPT of the derivatives could be inhibited by the enhanced molecular size.

Table 3 Dipole moment changes of the phototautomers of **C1** to **C4** during ESIPT

Compounds	E/Debye	E^*/Debye	K^*/Debye
C1	3.5310	3.5467	7.6134
C2	4.6885	4.8772	8.8682
C3	4.4019	4.7216	7.2821
C4	3.5456	3.5508	7.5122

Frontier Orbital and Electronic Transition

The electron cloud density in the frontier orbital of E and E^* is presented in Fig. 2. An π symmetry in HOMO, LUMO and LUMO + 1 orbital of the derivatives suggests that the absorption and normal emission spectra of **C1**–**C4** is original from (π, π*) electron transition. Figure 2 shows that the electron cloud density in HOMO orbital of E and E^* is distributed mainly in chromophore part, and it locates mainly in 2-(2-hydroxy-phenyl)-benzotriazole segment in LUMO orbital. In contrast, the major electron cloud density

Table 4 Main peaks of the absorption and normal emission spectra (λ), oscillator strengths (*f*) and the excitation weightages of the derivatives **C1** to **C4**

Compounds	Absorption			Normal emission		
	λ/nm	*f*	Composition	λ/nm	*f*	Composition
C1	306.3	1.1787	H-0→L + 1 (+80%)	375.1	1.3770	H-0→L + 1 (+72%)
C2	306.1	1.1712	H-0→L + 1 (+80%)	378.1	1.3395	H-0→L + 1 (+72%)
C3	336.3	1.4417	H-0→L + 1 (+67%)	398.4	1.6054	H-0→L + 1 (+74%)
C4	367.9	1.1870	H-0→L + 1 (+88%)	429.3	1.6664	H-0→L + 1 (+77%)

Table 5 Energy levels of HOMO, LUMO, LUMO + 1 in the derivatives **C1** to **C4**

		HOMO	LUMO	LUMO + 1	$\Delta E_{HOMO-LUMO}$/ev	$\Delta E_{HOMO-LUMO+1}$/ev
C1	E	−5.3512	−1.8664	−1.0354	−3.4848	−4.3158
	E^*	−4.8584	−1.8947	−1.5323	−2.9637	−3.3261
	K^*	−4.9892	−2.6025	−1.0052	−2.3867	−3.9840
C2	E	−5.4094	−1.8877	−1.0893	−3.5217	−4.3201
	E^*	−4.8965	−1.9152	−1.5938	−2.9813	−3.3027
	K^*	−5.0181	−2.6139	−1.0613	−2.4042	−3.9568
C3	E	−4.6336	−1.8096	−0.6588	−2.8240	−3.9748
	E^*	−4.2623	−1.8030	−1.0841	−2.4593	−3.1782
	K^*	−4.6075	−2.5503	−0.6291	−2.0572	−3.9784
C4	E	−4.8140	−1.8558	−1.0408	−2.9582	−3.7732
	E^*	−4.4532	−1.8534	−1.4003	−2.5998	−3.0529
	K^*	−4.7985	−2.5914	−1.0082	−2.2071	−3.7903

is distributed in chromophore part of LUMO + 1 orbital. The results indicate that the absorption and normal emission is characterized with internal charge transfer nature. It is obvious that the overlapping extent of HOMO/LUMO + 1 is larger than that of HOMO/LUMO.

Figure 2 shows that the electron density distribution mainly locates at chromophore part in K^*, and 2-(2-hydroxy-phenyl)-benzotriazole segment has negligible electron cloud density distribution. This means that the internal proton transfer in the excited state is lack of enough original electron driving force. As a consequence, the possibility of internal proton transfer could be diminished in the excited state. This also explains why the structural parameters of these derivatives display small change as excitation.

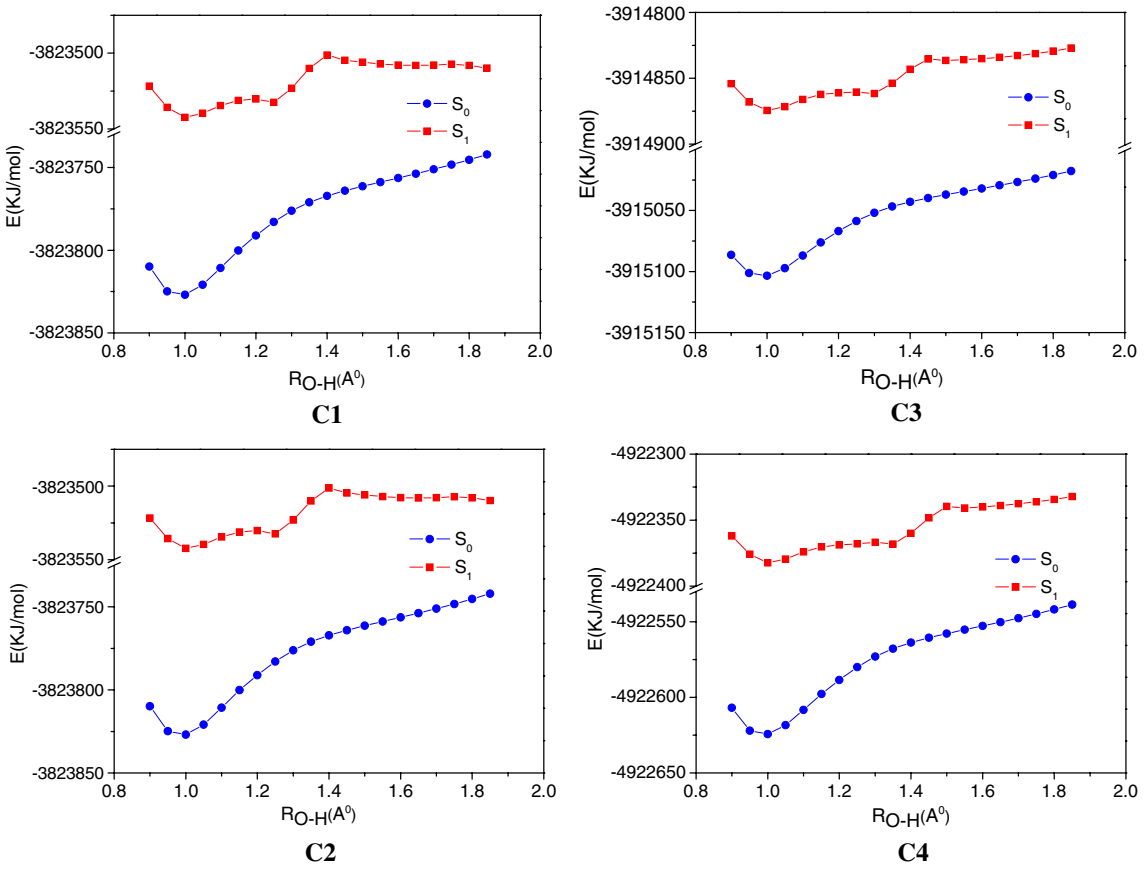

Fig. 3 Potential energy curves of the internal proton transfer with O–H distance (R_{O-H}) in S_0 and S_1 of **C1**–**C4**

We further calculated the Mulliken charge distribution of the atoms associated with ESIPT ($\mathbf{N_1}$, $\mathbf{H_6}$, $\mathbf{O_5}$, Fig. 1). For a typical ESIPT molecule, proton transfers from hydroxy to amino group as E is excited. This causes the enhancement of negative charge in proton-donor atom, and the increasing positive charge in proton-receptor atom. Consequently, the alkalinity of proton-donor is increased and the acidity of proton-receptor is increased during ESIPT. However, Table 2 shows that for **C3** and **C4**, the charges in the three atoms do not exhibit any change as E is excited to E^*, which is quite similar to the structural parameter changes. In contrast, the charges of $\mathbf{O_5}$ and $\mathbf{N_1}$ atoms show some changes for **C1** and **C2**, though it is small (0.001 eV). The data suggest that the possibilities of ESIPT occurrence could be small for all the derivatives. On the other hand, **C1** and **C2** could have a larger possibility to undergo ESIPT than **C3** and **C4**. This also interpret that **C1** and **C2** exhibits larger dipole moment changesthan **C3** and **C4** from E^* to K^* (Table 3).

The data in Table 4 demonstrate further that the absorption of **C1**–**C4** is mainly from the electron transition of HOMO→LUMO + 1 because such transition has larger oscillator strengths and higher excitation weightages than HOMO→LUMO. As a result, the normal emission of **C1**–**C4** is from the electron decay of LUMO + 1→HOMO. The calculation also shows that the energy gaps of HOMO-LUMO and HOMO-LUMO + 1 of **C1** and **C2** are greater than those of **C3** and **C4** respectively (Table 5). Consequently, the maximal absorption wavelength and normal emission wavelength of **C1** and **C2** are red-shifted to those of **C3** and **C4** respectively (Table 5).

Potential Energy Curves

Figure 3 shows the potential energy curves of the internal proton transfer with O–H distance (R_{O-H}) in S_0 and S_1 states. **C1**–**C4** exhibit a minimal energy position at 1.0 Å (R_{O-H}) in S_0 and S_1, which represents the stable E form.

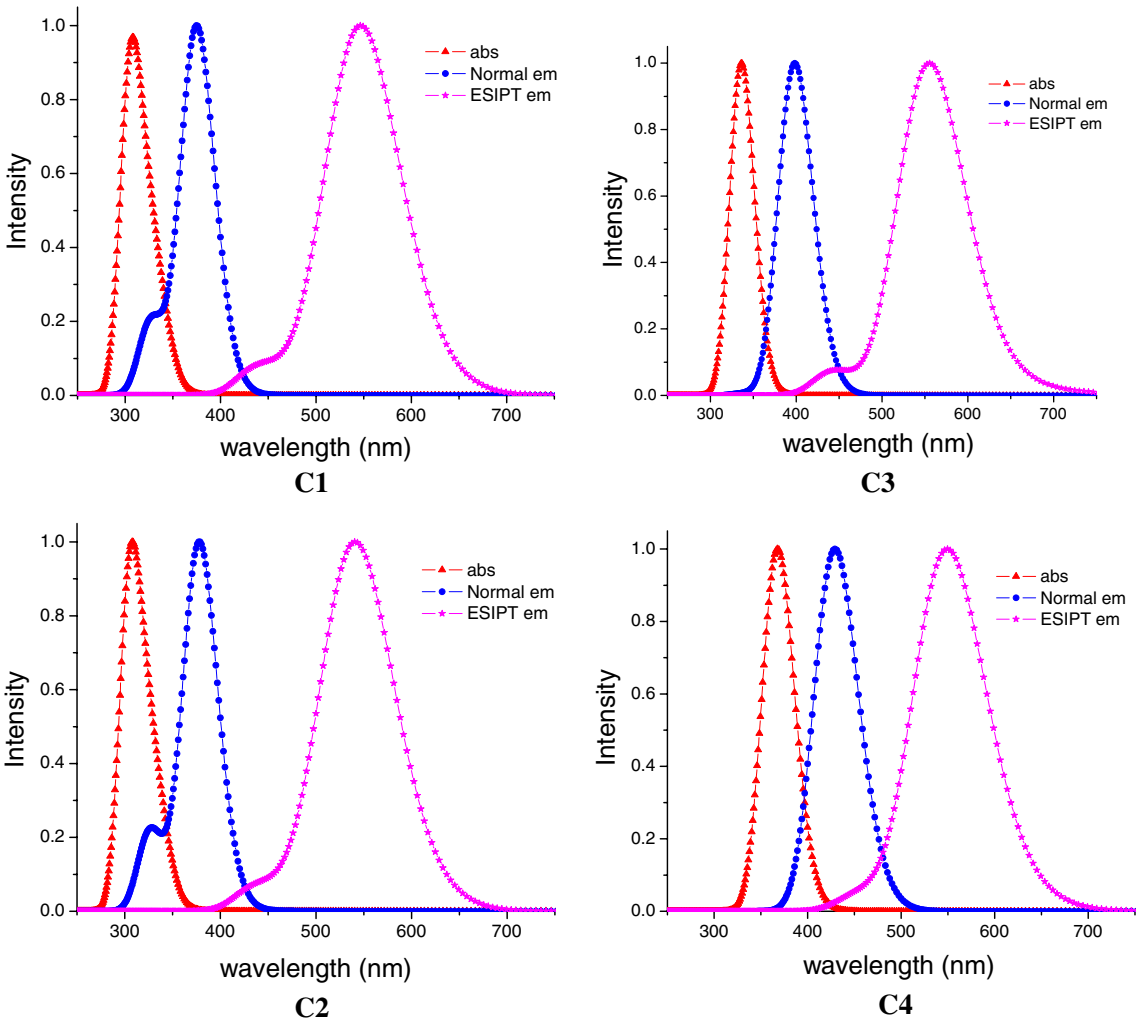

Fig. 4 Calculated absorption spectra, normal emission spectra, and ESIPT spectra of **C1** to **C4**

While, the energy keeps increasing with further extension of R_{O-H} in S_0. In contrast, the energy barrier appears in S_1 of **C1**–**C4** as R_{O-H} is further increased. The results demonstrate that stable K form does not exist in the ground states of **C1**–**C4**, while it exists in the excited state. As discussed, the molecular geometry optimization also shows that no stable K form could be obtained. This suggests that **C1**–**C4** could not undergo internal proton transfer in the ground state.

Furthermore, the potential energy curves of **C1** and **C2** display remarkably different change tendency from those of **C3** and **C4** in S_1. The energy of **C1** and **C2** tends to decrease while it passes through the energy barrier, while the energy of **C3** and **C4** keep increasing with R_{O-H} even as it gets over the energy barrier. The results demonstrate that the potential energy curves of ESIPT in **C1**–**C4** could be tuned by the variation of electron donor or acceptor group in chromophore part, and **C1** and **C2** could undergo ESIPT more easily than **C3** and **C4**.

In general, the relationship between ESIPT and its energy barrier has three different situations: (1) molecules can undergo ESIPT without a barrier between the normal tautomer (enol) and the proton transfer tautomer (keto), which have the energy order as ($E_{enol} < E_{keto}$) < ($E^*_{keto} < E_{enol}^*$); (2) ESIPT could occur with a barrier between enol and keto tautomers, which have the energy order is ($E_{enol} < E_{keto}$) < ($E^*_{keto} \approx E_{enol}^*$);(3) the energy order is ($E_{enol} < E_{keto}$) < ($E^*_{enol} < E^*_{keto}$), ESIPT cannot take place. In the present study, **C1**–**C4** exhibit remarkably large energy barrier (~ 40 KJ/mol), and $E^* \rightarrow K^*$ is a typical endothermic process. Hence, **C1**–**C4** could have small possibility to undergo ESIPT. As shown in Fig. 2, HOMO and LUMO electron densities are localized at different parts of the molecule. Even though the two moieties are connected through an oxo-bridge, the conjugated pi-electrons are separated at the two parts of the molecules. We assume that if two parts are connected with via C–C conjugated double bonds, the energy barriers of ESIPT could be decreased, and ESIPT could be easier to take place.

Figure 4 shows that ESIPT emission of **C1**–**C4** are red-shifted largely to those of normal emission. Furthermore, the red-shifts of **C3** and **C4** are smaller than those of **C1** and **C2**. This in turn indicates that it is more difficult for **C3** and **C4** to undergo ESIPT than for **C1** and **C2**.

Conclusions

The calculation of structural parameters, Mulliken charge and the electron density distribution of E and K in S_0 and S_1 suggests that it could be difficult to undergo ESIPT for these derivatives. The calculation demonstrates that the increased molecular size could play some negative role on ESIPT. On the other hand, the derivatives with electron acceptor groups show greater chance to undergo ESIPT than the derivatives with electron donor groups. Electron density distribution demonstrates that the conjugated pi-electrons are separated by single oxo-bridge. This indicates that C–C double bridging bonds could be more beneficial for ESIPT. The calculation demonstrates if ESIPT occurs, the derivatives emit an obvious ESIPT fluorescence with large Stokes red-shift. The results presented in this article would be beneficial for the construction of new ESIPT compounds for various use.

Acknowledgements The authors would thank National Natural Science Foundation of China (Nos. 20776165, 20702065 and 20872184) and Natural Science Foundation of CQ CSTC (Nos. CSTC, 2010BB0216) for financial supports. The authors appreciate for the support from the Key Foundation of Chongqing Science and Technology Commission (CSTC 2008BA4020). We appreciate financial supports from the Fundamental Research Funds for the Central Universities (No. CDJZR10220006, CDJXS10221137, CDJZR10225501).

References

1. Ogawa AK, Abou-Zied OK, Tsui V, Jimenez R, Case DA, Romesberg FE (2000) A phototautomerizable model DNA base pair. J Am Chem Soc 122:9917–9920. doi:10.1021/ja001778n
2. Abou-Zied OK, Jimenez R, Romesberg FE (2001) Tautomerization dynamics of a model base pair in DNA. J Am Chem Soc 123 (19):4613–4614. doi:10.1021/ja003647s
3. Rodembusch FS, Campo LF, Stefani V, Rigacci A (2005) The first silica areogels fluorescent by excited state intramolecular proton transfer mechanism(ESIPT). J Mater Chem 15:1537–1541. doi:10.1039/b416958a
4. Lim SJ, Seo J, Soo YP (2006) Photochromic switching of excited-State intramolecular proton-transfer (ESIPT) fluorescence: a unique route to high-contrast memory switching and nondestructive readout. J Am Chem Soc 128(45):14542–14547. doi:10.1021/ja0637604
5. Cardoso MB, Samios D, Silveira NP, Rodembusch FS, Stefani V (2007) ESIPT-exhibiting protein probes: a sensitive method for rice proteins detection during starch extraction. Photochem Photobiol Sci 6(1):99–102. doi:10.1039/b610999c
6. Mutai T, Tomoda H, Ohkawa T, Yabe Y, Araki K (2008) Switching of polymorph-dependent ESIPT luminescence of an imidazo[1, 2-a]pyridine derivative. Angew Chem Int Ed 47 (49):9522–9524. doi:10.1002/anie.200803975
7. Chou PT, Huang CH, Pu SC, Cheng YM, Liu YH, Wang Y, Chen CT (2004) Tuning excited-state charge/proton transfer coupled reaction via the dipolar functionality. J Phys Chem A 108 (31):6452–6454. doi:10.1021/jp0476390
8. Yu WS, Cheng CC, Cheng YM, Wu PC, Song YH, Chi Y, Chou PT (2003) Excited-state intramolecular proton transfer in five-membered hydrogen-bonding systems: 2-pyridyl pyrazoles. J Am Chem Soc 125:10800–10801. doi:10.1021/ja035382y
9. Chen CL, Lin CW, Hsieh CC, Lai CH, Lee GH, Wang CC, Chou PT (2009) Dual excited-state intramolecular proton transfer reaction in 3-hydroxy-2-(pyridine-2-yl)-4H-chromen-4-one. J Phys Chem A 113:205–214. doi:10.1021/jp809072a
10. Chen KY, Hsieh CC, Cheng YM, Lai CH, Chou PT (2006) Extensive spectral tuning of the proton transfer emission from 550 to 675 nm via a rational derivatization of 10-hydroxybenzo[h] quinoline. Chem Commun 4395–4397. doi:10.1039/b610274c

11. Chen KY, Cheng YM, Lai CH, Hsu CC, Ho ML, Lee GH, Chou PT (2007) Ortho green fluorescence protein synthetic chromophore; excited-state intramolecular proton transfer via seven-membered-ring hydrogen-bonding system. J Am Chem Soc 129:4534–4535. doi:10.1021/ja070880i
12. Seo J, Kim S, Park SY (2004) Strong solvatochromic fluorescence from the intramolecular charge-transfer state created by excited-state intramolecular proton transfer. J Am Chem Soc 126 (36):11154–11155. doi:10.1021/ja047815i
13. Sakai K, Ichikawaa M, Taniguchi Y (2006) Photoluminescent mechanism of a proton-transfer laser dye in highly doped polymer films. Chem Phys Lett 420:405–409. doi:10.1016/j.cplett.2005.12.074
14. Kim TI, Kang HJ, Han G, Chung SJ, Kim Y (2009) A highly selective fluorescent ESIPT probe for the dual specificity phosphatase MKP-6. Chem Commun 5895–5897. doi:10.1039/B911145J
15. Zhang H, Han LF, Zachariasse KA, Jiang YB (2005) 8-hydroxyquinoline benzoates as highly sensitive fluorescent chemosensors for transition metal ions. Org Lett 7(19):4217–4220. doi:10.1021/ol051614h
16. Sun WH, Li SY, Hu R, Qian Y, Wang SQ, Yang GQ (2009) Understanding solvent effects on luminescent properties of a triple fluorescent ESIPT compound and application for white light emission. J Phys Chem A 113(20):5888–5895. doi:10.1021/jp900688h
17. Park S, Kwon OH, Kim S, Park S, Choi MG, Cha M, Park SY, Jang DJ (2005) Imidazole-based excited-state intramolecular proton-transfer materials: synthesis and amplified spontaneous emission from a large single crystal. J Am Chem Soc 127 (28):10070–10074. doi:10.1021/ja0508727
18. Paterson MJ, Robb MA, Blancafort L, DeBellis AD (2004) Theoretical study of benzotriazole UV photostability: ultrafast deactivation through coupled proton and electron transfer triggered by a charge-transfer state. J Am Chem Soc 126(9):2912–2922. doi:10.1021/ja0386593
19. Frisch MJ, Trucks GW, Schlegel HB, Scuseria GE, Robb MA, Cheeseman JR, Montgomery JA, Vreven T, Kudin KN, Burant JC, Millam JM, Iyengar SS, Tomasi J, Barone V, Mennucci B, Cossi M, Scalmani G, Rega, N, Petersson GA, Nakatsuji H, Hada M, Ehara M, Toyota K, Fukuda R, Hasegawa J, Ishida M, Nakajima T, Honda Y, Kitao O, Nakai H, Klene M, Li X, Knox JE, Hratchian HP, Cross JB, Bakken V, Adamo C, Jaramillo J, Gomperts R, Stratmann RE, Yazyev O, Austin AJ, Cammi R, Pomelli C, Ochterski JW, Ayala PY, Morokuma K, Voth GA, Salvador P, Dannenberg JJ, Zakrzewski VG, Dapprich S, Daniels AD, Strain MC, Farkas O, Malick DK, Rabuck AD, Raghavachari K, Foresman JB, Ortiz JV, Cui Q, Baboul AG, Clifford S, Cioslowski J, Stefanov BB, Liu G, Liashenko A, Piskorz P, Komaromi I, Martin RL, Fox DJ, Keith T, Al-Laham MA, Peng CY, Nanayakkara A, Challacombe M, Gill PMW, Johnson B, Chen W, Wong MW, Gonzalez C, Pople JA, Gaussian 03, Revision B.03.
20. Zgiershi MZ, Grabowska A (2000) Photochromism of salicylideneaniline (SA). How the photochromic transient is created: a theoretical approach. J Chem Phys 112(14):6329–69367. doi:10.1063/1.481194
21. Liang YP, Cao YH (2005) Intramolecular proton or hydrogen-atom transfer in the ground- and excited-states of 2-hydroxybenzophenone: a theoretical study. Chem Phys 315(3):297–302. doi:10.1016/j.cplett.2007.03.010
22. Liang YH, Yi PG (2007) Theoretical studies on structure, energetic and intramolecular proton transfer of alkannin. Chem Phys Lett 438(4–6):173–177. doi:10.1016/j.cplett.2007.03.010
23. Yang ZN, Yang SY, Zhang JP (2007) Ground- and excited-state proton transfer and rotamerism in 2-(2-Hydroxyphenyl)-5-phenyl-1, 3, 4-oxadiazole and its O/"NH or S"-substituted derivatives. J Phys Chem A 111(28):6354–6360. doi:10.1021/jp068589x
24. Gaenko AV, Devarajan A, Tselinskii IV, Ryde U (2006) Structural and photoluminescence properties of excited state intramolecular proton transfer capable compounds—potential emissive and electron transport materials. J Phys Chem A 110 (25): 7935–7942 doi:10.1021/jp060646z
25. Gorelsky SI Swizard program, revision XX, http://www.sg-chem.net/
26. Wang Y, Wu G (2008) Electronic structure characteristics of ESIPT and TICT fluorescence emissions and calculations of emitting energies. Acta Phys–Chim Sim 24:552–560, in Chinese